Distribution Agreement

In presenting this thesis as a partial fulfillment of the requirements for a degree from Emory University, I hereby grant to Emory University and its agents the non-exclusive license to archive, make accessible, and display my thesis in whole or in part in all forms of media, now or hereafter now, including display on the World Wide Web. I understand that I may select some access restrictions as part of the online submission of this thesis. I retain all ownership rights to the copyright of the thesis. I also retain the right to use in future works (such as articles or books) all or part of this thesis.

Maddie Lampert April 9, 2025

Source of Calcium Transients Involved in Synaptic Scaling in the Chick Embryo

by

Maddie Lampert

Dr. Peter Wenner
Adviser

Neuroscience & Behavioral Biology

Dr. Peter Wenner

Adviser

Dr. Andrea Roeser

Committee Member

Dr. Victor Faundez

Committee Member

2025

Source of Calcium Transients Involved in Synaptic Scaling in the Chick Embryo

By

Maddie Lampert

Dr. Peter Wenner
Adviser

An abstract of
a thesis submitted to the Faculty of Emory College of Arts and Sciences
of Emory University in partial fulfillment
of the requirements of the degree of
Bachelor of Science with Honors

Neuroscience & Behavioral Biology

2025

Abstract

Source of Calcium Transients Involved in Synaptic Scaling in the Chick Embryo
By Maddie Lampert

Background: Homeostatic plasticity describes the set of mechanisms that act to ensure neurons maintain appropriate levels of excitability amidst chronic perturbations. Deficits in homeostatic plasticity have been proposed to be implicated in a range of nervous system disorders including autism spectrum disorders. It has been previously established that rapid homeostatic synaptic scaling in the chick embryo is mediated by NMDA receptor activation associated with miniature postsynaptic currents (mPSCs), but the downstream substrate that triggers a change in postsynaptic current amplitude remains unknown. Recent evidence suggests calcium as the key substrate, but this theory has not yet been investigated in the chick embryo, and the source of calcium has not been identified.

Methods: Motor neurons from the embryonic chick spinal cord were labeled with cytoplasmic and mitochondrial calcium indicators and imaged in TTX before, during, and after treatment with AMPA, NMDA, and GABA receptor antagonists to quantify the frequency of mini-induced calcium transients.

Results: Data from a total of 6 cords filled with Calcium Green Dextran and 3 cords electroporated with mito-GCaMP6F were collected and included in the analysis. The frequency of cytoplasmic, but not mitochondrial, calcium transients decreased in the presence of the antagonists.

Conclusion: This is the first study to investigate calcium transients induced by miniature post-synaptic currents in embryonic chick spinal motorneurons. The significant reduction of cytoplasmic calcium fluorescence upon inhibition of mPSCs provides further evidence that one, all, or a combination of these receptors serve as essential sources of calcium in this system. Future studies should build upon these findings to identify the specific source of calcium and its downstream effects that induce scaling.

Source of Calcium Transients Involved in Synaptic Scaling in the Chick Embryo

By

Maddie Lampert

Dr. Peter Wenner
Adviser

A thesis submitted to the Faculty of Emory College of Arts and Sciences
of Emory University in partial fulfillment
of the requirements of the degree of
Bachelor of Science with Honors

Neuroscience & Behavioral Biology

2025

Acknowledgements

Thank you to my mentor, Dr. Peter Wenner, for believing in me and teaching me the skills I have now. I appreciate all the time and energy you have put into my success and the success of this project. Our many theoretical conversations have been beyond insightful and intellectually stimulating. You have fueled my curiosity and love for science.

Thank you to the rest of the Wenner lab, especially Dr. Dobromila Pekala and Dr. Carlos Gonzales-Islas for your day-to-day assistance and company in lab. Thank you to Izzy Witteveen for teaching me how to electroporate and for your wisdom during the PhD application process.

Thank you to my NBB professors, including but not limited to Dr. Andrea Roeser, Dr. Leah Roesch, Dr. Alex Grizzell, Dr. Patrick Cafferty, and Dr. Gillian Hue for providing me with the foundational knowledge I will take with me for the rest of my career, and for being my academic and professional cheerleaders throughout my Emory experience. I appreciate the space you have provided to ask endless questions, as well as the wisdom and guidance you have provided as I decide on the next steps of my research journey. I will miss eating lunch and chatting in the NBB suite.

Thank you to Dr. David Goldsmith, who saw my potential and provided invaluable mentorship as I began my research journey.

Thank you to my parents, who always supported my academic and creative pursuits.

Thank you to my cats for providing much needed stress relief and entertainment.

Table of Contents

Introduction & Background ……1

Figure 1 - Effect of Ru265 on mitochondrial calcium fluorescence…….…...…5

Research Question and Hypothesis……..……6

Methods…….…….....7

Figure 2 – Embryonic development and tissue preparation timeline……..…8

Figure 3 – Chick embryo spinal cord……..……9

Figure 4 – Calcium imaging snapshots…….…….…….……..11

Results …….……...……..12

Figure 5 – Cytoplasmic and mitochondrial calcium in spinal motor neuron dendrites…13

Figure 6 – Distribution of raw fluorescence values…….....13

Figure 7 – Representative ROI trace of cytoplasmic calcium fluorescence……..14

Figure 8 – Frequency of cytoplasmic calcium transients…….…….15

Figure 9 – Representative ROI trace of mitochondrial calcium fluorescence…….....16

Figure 10 – Frequency of mitochondrial calcium transients……...……..….17

Discussion…….…....18

Conclusion……21

References……..……22

Introduction and Background

Homeostatic plasticity describes the set of mechanisms that act to ensure neurons maintain appropriate levels of excitability amidst chronic perturbations. Deficits in homeostatic plasticity have been proposed to be implicated in a range of nervous system disorders, including Alzheimer's, drug addiction, autism spectrum disorders (ASD), Rett syndrome, and Fragile X (Kavalali & Monteggia, 2020; Frere & Slutsky, 2018; Pratt et al., 2011; Conrad et al., 2008; Südhof, 2008; Zoghbi, 2003; Blackman et al., 2012; Zhong & Chang, 2012; Zhang et al., 2018).

Homeostatic plasticity differs from Hebbian forms of plasticity, like long-term potentiation and long-term depression. Hebbian plasticity is determined by the timing and rate of synaptic spiking between the presynaptic and postysynaptic cell, while homeostatic plasticity is not dependent on the timing of spiking.

The current model of homeostatic plasticity involves a compensatory shift, increasing excitability after a period of low activity, or decreasing excitability after a period of heightened activity. The hypothesized mechanisms involve modifications in receptor type or conformation, channel expression, metabolism, and membrane potential.

In 1998, Gina Turiggiano found that complete inhibition of cell spiking using tetrodotoxin (TTX) resulted in a homeostatic compensation of quantal amplitude in postnatal rat visual cortical neurons in culture (Turiggiano et al., 1998). Following chronic TTX application, the amplitude of miniature excitatory postsynaptic currents (mEPSCs, or 'minis') induced by a single vesicle release increased, indicating an adjustment in excitability. Further, chronically increasing activity levels by inhibiting Gamma-Aminobutyric Acid (GABA) receptors decreased mEPSC amplitude and excitability, while inhibiting glutamatergic signaling through alpha-amino-3-hydroxy-5-methyl-4-isoxazolepropionate (AMPA) receptors increased mEPSC

amplitude and excitability (Turiggiano et al., 1998). Of note, Turiggiano found that N-methyl-d-aspartate (NMDA) inhibition resulted in no change in firing rate or mEPSC amplitude. This was the first paper to identify bidirectional scaling of mEPSC amplitudes in the absence of spiking.

In embryonic chick spinal motorneurons, inhibition of cell spiking also results in scaling of mEPSCs (Gonzales-Islas, 2006). The compensation in excitability is seen after 2 days of lidocaine infusion *in vivo.* Additionally, decreasing activity by reducing GABAergic transmission (depolarizing and excitatory at this point in chick development) similarly triggers a compensatory increase in mEPSC amplitude at the 2-day timescale (Wilhelm & Wenner, 2008). In contrast, direct inhibition of NMDA receptors (NMDARs) in the absence of spiking resulted in rapid adjustment of mEPSC amplitude 1-3 hours after blockade (Pekala & Wenner, 2022). Blocking spiking activity alone does not trigger scaling within 3 hours, suggesting that this rapid scaling is mediated by NMDA minis.

It is unclear whether these rapid and slow forms of scaling act through the same pathway. It is possible that in the slow form of scaling, activity blockade causes a downstream reduction in NMDAR activity, triggering the same mechanism that acts during rapid scaling but at a slower rate. In the chick embryo, glutamatergic scaling is induced by blocking NMDA minis. The mechanism through which minis trigger scaling, however, remains unclear.

Both the slow and rapid forms of scaling involve the insertion of GluA2-lacking AMPAR subunits (Garcia-Bereguiain et al., 2013; Pekala & Wenner, 2022). These AMPARs are more permeable to calcium than GluA2-containing receptors and pass more current consistent with a homeostatic response to the perturbation. The critical role of localized calcium-permeable AMPAR subunits was first demonstrated by Sutton et al. (2006). Sutton et al. found that the rapid form of glutamatergic scaling requires the insertion of GluA2-lacking AMPARs (Sutton et al.,

2006). Inhibition of calcium-permeable AMPAR subunits prevented or reversed scaling induced by NMDA receptor blockade.

Reese and Kavalali (2015) further demonstrate that calcium transients induced by minis are critical for scaling. They were the first to use calcium imaging to visualize quantal NMDA-induced calcium transients. They found that in mice and rat hippocampal cultures, mini spontaneous calcium transients (mSCTs) were dependent on NMDAR activity but not L-type voltage-gated calcium channels or AMPARs. Further, Aoto et al. (2008) showed that inhibition of NMDAR mPSC activity results in scaling via calcium-induced disinhibition of retinoic acid synthesis (Aoto et al., 2008). Together, these findings suggest that local calcium entry through NMDARs induces multiple pathways that prevent an increase in calcium-permeable AMPARs in hippocampal cultures.

The signaling pathway from calcium entry to receptor insertion and scaling remains mostly unknown. Calcium could be entering the cell through multiple paths, including via voltage-gated calcium channels upon depolarization by GABAR activation or via NMDARs upon depolarization by AMPAR activation. Upon entering the cell, calcium could interact with kinases and other proteins in the cytoplasm, or it could travel to the mitochondria where it is taken up by the mitochondrial calcium uniporter (MCU).

In recent years, mitochondria have arisen as a potential mediator of homeostatic scaling by acting as a calcium sensor. Styr & Slutsky (2019) found that inhibiting mitochondrial di-hydroorate dehydrogenase (DHODH) decreased firing rate set point and mEPSCs in hippocampal cultures. Further, Pekala (unpublished) demonstrated that reducing mitochondrial calcium via the MCU-antagonist Ruthenium (Ru265) triggered scaling in chick embryo spinal

motoneurons. Little else is known about the role of mitochondria in homeostatic plasticity, motivating our investigation of mitochondrial calcium transients.

Preliminary results from the current study validated the function of the mitochondrial calcium fluorescence indicator, mito-GCaMP6f, in this system. Upon a spontaneous or stimulated burst of network activity, voltage peaks in the ventral root coincide with increased cytoplasmic calcium fluorescence, which is then followed by a delayed but sustained peak in mitochondrial calcium fluorescence (*Figure 1A*). Additionally, the magnitude of mitochondrial calcium fluorescence is significantly reduced in the presence of the MCU inhibitor Ru265 (*Figure 1B*).

No studies have yet visualized quantal calcium transients in embryonic chick motor neurons or investigated their response to receptor blockade. Development of this technique will provide a tool to figure out the key downstream effects of calcium transients in scaling.

A deeper understanding of the functions of NMDAR-mediated mPSC signaling could provide beneficial therapeutic strategies. The NMDA antagonist, ketamine, has shown rapid antidepressant effects in people with treatment-resistant depression (Newport et al., 2015). However, the link between NMDA-dependent scaling and the beneficial antidepressant effects of ketamine remains unclear. Further understanding of the downstream effects of NMDAR activation on synaptic modulation is necessary.

Homeostatic plasticity is also critical in controlling the strength of both inhibitory and excitatory components of networks during the construction of brain circuits. Disruption of the excitatory/inhibitory balance during critical periods of development may contribute to the wide variety of phenotypes exhibited in ASD (Gogolla et al., 2009). One early phenotype of ASD is poor gross motor function and/or atypical sensory and motor behaviors, suggesting a possible

role of the spinal cord in the pathophysiology of the disorder (Lim et al., 2021). However, research and diagnostic efforts focus largely on later-emerging behavioral phenotypes. Here, we will assess cellular dynamics that likely play a role in the establishment and fine-tuning of motor circuits and behaviors.

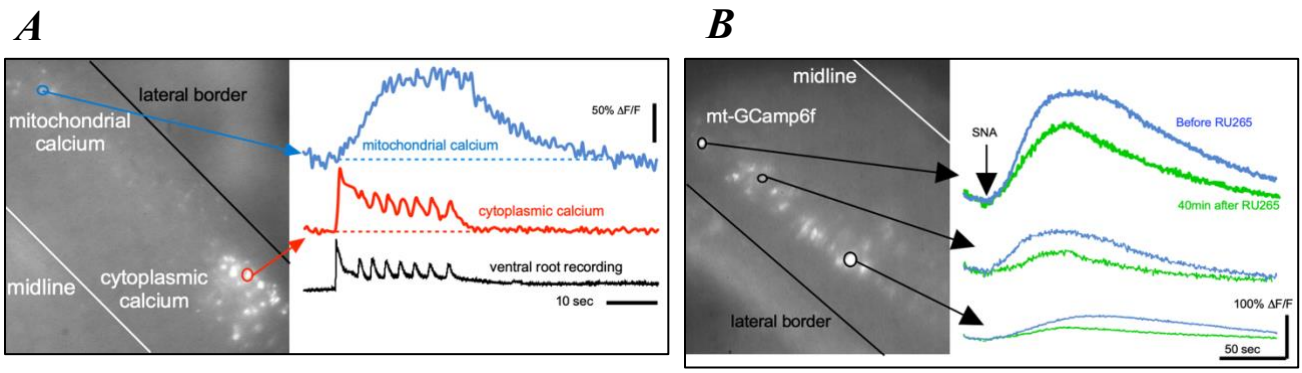

Figure 1 – Effect of Ru265 on mitochondrial calcium fluorescence
A) Calcium fluorescence imaging performed on whole tissue of embryonic (E10) chick spinal cord labeled with mito-GCaMP6f and Calcium Green Dextran. Spiking of cytoplasmic calcium coincides with voltage recordings from the ventral root, followed by a larger gradual increase of mitochondrial calcium fluorescence. B) The magnitude of mitochondrial calcium fluorescence induced by a burst of spontaneous network activity is significantly reduced after the application of Ru265.

Research Question and Hypothesis

Research Question: Can we identify calcium transients dependent on mPSCs that could underly scaling in the chick embryo spinal cord?

Hypothesis: Detected calcium transients are dependent on mPSCs.

Aim 1*:* Develop a technique to identify and characterize quantal post-synaptic calcium transients in the cytoplasm and mitochondria of developing chick motoneurons.

Aim 2*:* Test that these calcium transients are reduced when blocking mPSCs.

Methods

Segments of the embryonic chick spinal cord were labeled with a cytoplasmic or mitochondrial calcium indicator, sliced transversely, and imaged in TTX and a 0 Magnesium solution before, during, and after treatment with AMPAR, NMDAR, and GABAR antagonists to quantify the frequency of mini-induced calcium transients.

Tissue Preparation

The model used in these experiments is the embryonic chick spinal cord. Eggs were received on Mondays from Hyline Hatcheries and incubated at 36ºC. Embryos were incubated until embryonic day 10 (E10/Hamburger Hamilton Stage 36) (Hamburger & Hamilton, 1951). At this point in chick development, central afferents have reached the gray matter of the spinal cord, motoneurons have reached their muscle targets, and the limbs exhibit spontaneous, irregular, jerky movements (Wenner, 2020).

Some embryos were injected *in ovo* with a plasmid carrying the mitochondrial calcium indicator, mito-GCaMP6F (Ashrafi et al., 2020), at E3 in the neural tube and electroporated. These embryos were placed back in the incubator to develop until E10 (*Figure 2*).

The dissection was performed at E10 in Tyrode's solution (139mM NaCl, 12mM D-glucose, 17 mM $NaHCO_3$, 3 mM KCl, 1mM $MgCl_2$, 3 mM $CaCl_2$) with oxygen flow (95% O2/5% CO2) at 14-15ºC. The dissection involved eviscerating the embryo, removing the rostral half, cutting off the front plate of the spine, and extracting the spinal cord.

Isolated cords that were not previously electroporated were retrogradely labeled in the lumbosacral region with Calcium Green Dextran, a cytoplasmic calcium indicator. Isolated cords were allowed to retrogradely transport the indicator to the cell body overnight at 17-18ºC.

In a few early experiments, the whole nerve was filled (*Figure 3*). This resulted in weaker labeling of motoneuron dendrites due to the greater distance the dye had to travel. We then adjusted the filling procedure to isolate and fill the ventral root, which was closer to the cell bodies (*Figure 3*), thereby providing stronger labeling of the motoneuron dendrites in comparison to the background.

We began imaging the whole tissue without slicing the spinal cord. This preparation allowed us to visualize individual cell bodies, but not dendrites (*Figure 4A*). The shift to transverse slices provided sufficient resolution to record from independent puncta on multiple dendrites within one frame of view (*Figure 4B).* The tissue was sliced the morning after dissection using a vibratome (Leica VT 1000S) to make slices of 250-300 microns. Slices were placed in a bath of Tyrode's solution bubbled with 95% O2 and 5% CO2.

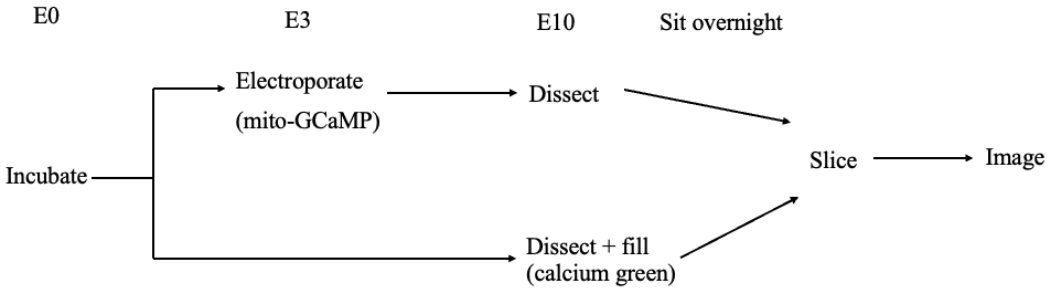

Figure 2 – Embryonic development and tissue preparation timeline

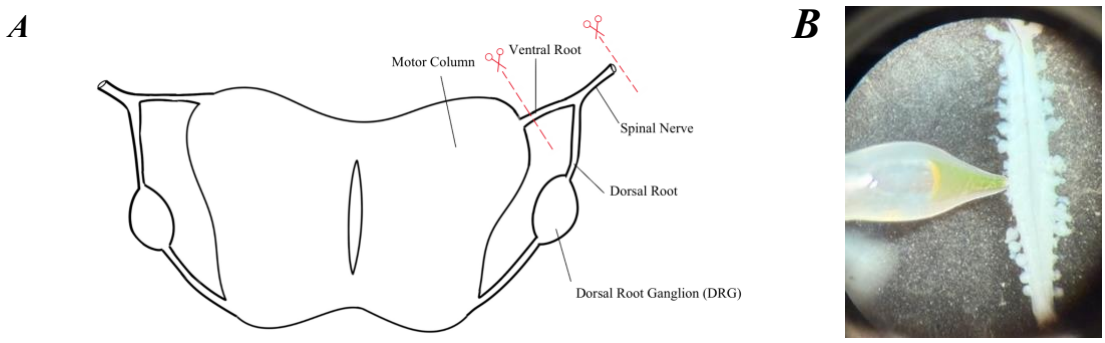

Figure 3 – Chick embryo spinal cord
A) Illustration of a transverse cross-section of the chick spinal cord. Note the two cutting sites – one more lateral, including the whole spinal nerve, and one more medial, including the ventral root (consisting of efferent motor neurons) but excluding the dorsal root (sensory neurons). B) Image of isolated spinal cord after dissection. A ventral root from the lumbosacral region is suctioned and infused with Calcium Green Dextran. A-B) The dye is retrogradely transported from axons in the ventral root medially to the cell bodies and dendrites located in the motor column.

Calcium Imaging

All calcium imaging was performed using a Xenon Arc Lamp (Olympus). Slices were visualized at baseline to identify an optimal region of interest with prominently labeled dendrites compared to background fluorescence. The image was viewed through a 40x objective, and camera intensification was adjusted to take advantage of the full dynamic range of the camera (Stanford Photonics XR/ABF). Exposure was limited using neutral density filters ranging from 0.7% to 6.0%.

Fluorescence was recorded in SimplePCI (HCImage) for periods of 2 minutes with a rolling average of 2-4 frames. This captured between 3.3-7.5 frames per second, providing between 400-900 frames per recording, with each frame representing 100-300ms. The temporal resolution varied with computer speed and storage. This range of resolution was sufficient to capture calcium transient events, which correlate with but last longer than the 100-500ms timescale of GABAergic and glutamatergic currents in this system.

Slices were housed in a chamber with modified Tyrode's solution, continuous oxygen flow and warmed to 27ºC. The modified Tyrode's solution (139 mM NaCl, 12mM D-glucose, 17 mM $NaHCO_3$, 3 mM KCl, 3 mM $CaCl_2$) excluded magnesium to increase baseline NMDAR calcium permeability. 1 uM Tetrodotoxin (TTX), an inhibitor of sodium channels, was added to inhibit spiking activity and visualize spontaneous mini-induced calcium currents.

After the characterization of baseline quantal calcium transients, AMPA, NMDA, and GABA receptor antagonists (10 uM CNQX, 50uM APV, 100 uM picrotoxin or bicuculline) were added to the bath solution for the "antagonists" condition. The tissue sat in the antagonist solution for 20-60 minutes before recording. The antagonist solution was then replaced with fresh 'modified' Tyrode's and TTX and given 30-60 minutes to wash out.

Data Analysis

Recordings were reviewed using FIJI (ImageJ) to calculate fluorescence values for each ROI for each frame of the 2-minute recording. 10-20 ROIs per recording were selected from dendritic puncta. The primary quantitative endpoint analyzed is the frequency of calcium transients per ROI per minute. This endpoint, calcium transient frequency, is compared between experimental groups. This protocol for quantifying calcium transients was adapted from Reese & Kavalali (2015).

The protocol for detecting and quantifying signals developed as experiments were conducted and analyzed. In the presented data, calcium transients are quantified as events in which the raw calcium fluorescence value was 2.6 standard deviations above the mean of the preceding 40 frames for 2 or more consecutive frames. 2 consecutive frames were required to exceed this threshold to avoid false positive detection from single-frame peaks due to noise.

In early analyses, a standard deviation of 2 and window size of 20 was used to calculate the threshold for significant events. The likelihood of the fluorescence of two frames in a row meeting criterion under this condition is 0.06%, and we successfully picked up signals. However, this method using 2 SDs produced many false positives, as significant events were detected in a non-biological fluorescence recording.

After adjusting the standard deviation threshold to 2.6 and the window size to 40, we detected consistently convincing events and reduced the frequency of false positives. The likelihood of these significant events resulting from random chance is only 0.002%. We also display the events identified by showing the plot of $\Delta F/F$ for each ROI.

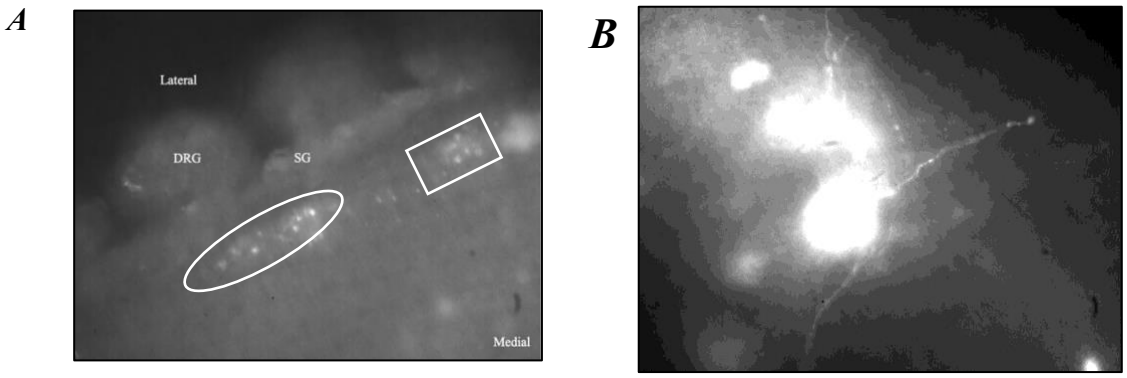

Figure 4 – Calcium imaging snapshots
A) Image of the ventral side of the whole spinal cord with in-tact dorsal root ganglion (DRG) and sympathetic ganglion (SG) with 20x objective. This cord was filled with cytoplasmic Calcium Green and expressed mitochondrial GCamp. The areas of increased luminescence show cytoplasmic calcium (boxed) and mitochondrial calcium (circled) in the cell bodies, but dendrites cannot be seen. B) Snapshot of 300-micron transverse cross-section viewed with 40x objective. The image is focused on a cluster of cells in the motor column. Note the bleached cell bodies but the visible dendritic branches and puncta with sufficient contrast with the background.

Results

Data from a total of 6 cords filled with Calcium Green and 3 cords electroporated with mito-GCaMP6f were collected and included in the analysis. For one cord, two series of experiments were conducted in the same preparation but in different regions. Experiments were conducted from October 2024 through January 2025. We were first able to visualize areas of increased fluorescence within the dendrites from both cytoplasmic and mitochondrial calcium in October (*Figure 5*). Data from all experiments followed a normal distribution (*Figure 6*).

The frequency of calcium transients was quantified as the average number of significant events (events in which the raw fluorescence value was 2.6 standard deviations above the mean of the preceding 40 frames for 2 or more consecutive frames) per ROI per minute. We were able to detect significant events in each included prep (preps with weak labeling and low contrast were excluded). In many cases, the frequency of events was reduced after the addition of the antagonists.

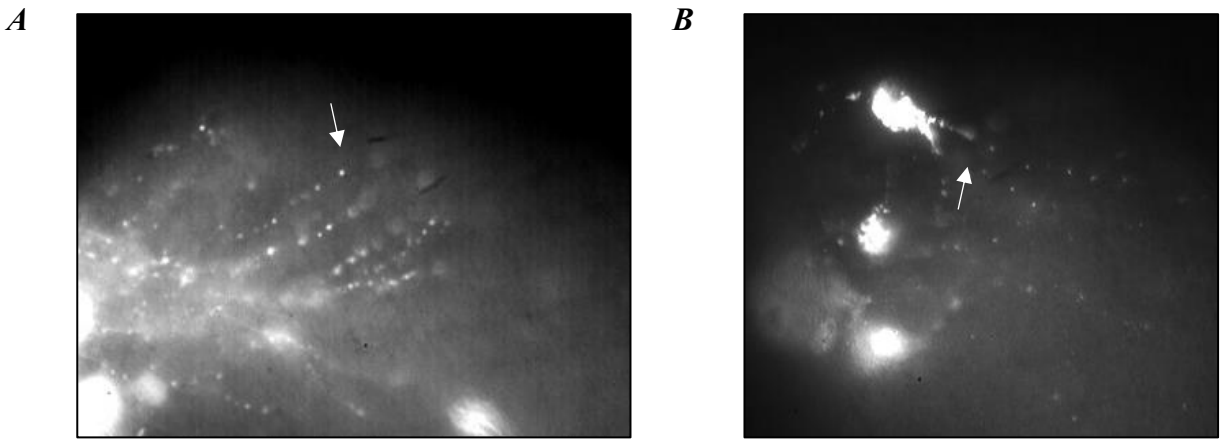

Figure 5 – Cytoplasmic and mitochondrial calcium in spinal motor neuron dendrites
A) Representative snapshot from successful fill of Calcium Green and imaging of cytoplasmic calcium in dendrites (transverse slice, 40x objective). Note the contrast in values between ROI of increased fluorescence (indicated with arrow, value = 78) and adjacent background (value = 34). B) Representative snapshot from successful electroporation of mito-GCaMP6f and visualization of mitochondrial calcium in dendrites (transverse slice, 40x objective). Note the contrast in values between ROI of increased fluorescence (indicated with arrow, value = 167) and adjacent background (value = 49).

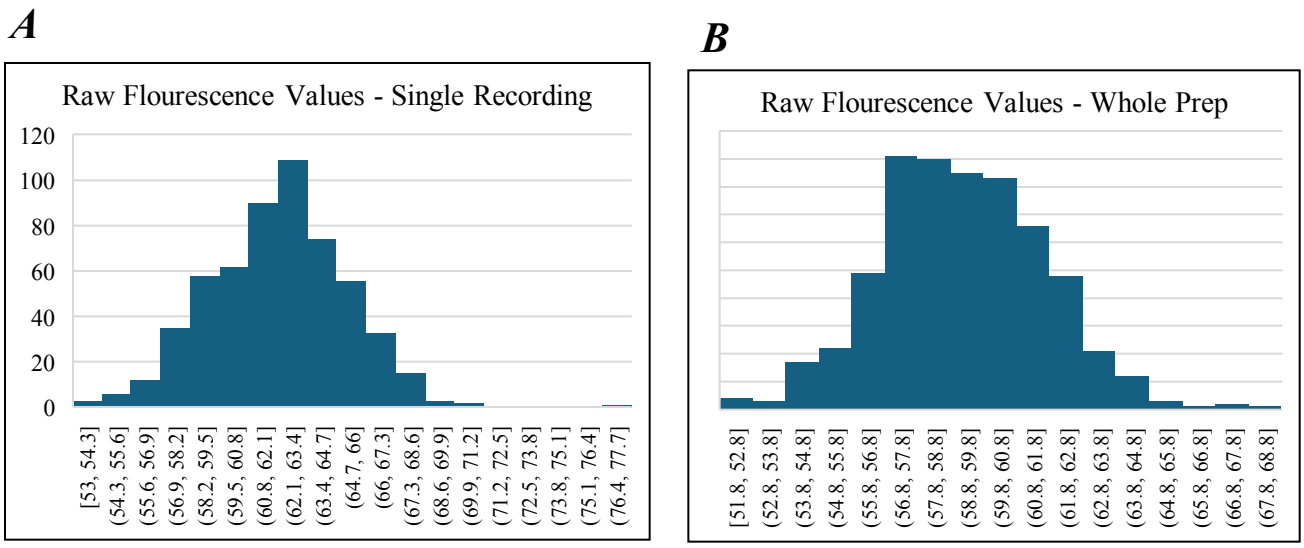

Figure 6 – Distribution of raw fluorescence values
A) Representative histogram of fluorescence values for all frames and all ROIs from one recording (mean: 62.3, median: 62.2, stdev: 3.04). B) Representative histogram of fluorescence values for all frames and all ROIs from all recordings from a single prep (mean: 81.8, median: 75.3, stdev: 29.5). Data from all experiments followed a normal distribution.

Cytoplasmic Calcium

7 trials were conducted using 6 cords that were retrogradely filled with Calcium Green and dendritic puncta were imaged for cytoplasmic calcium fluorescence transients (*Figure 7*). The average cytoplasmic calcium transient frequency at baseline was 0.040 ± 0.023 events per ROI per minute (*Figure 8*). An example trace of calcium fluorescence over a 2-minute period is shown in *Figure 7* where one event reaches the threshold for being considered a calcium triansient. 30-60 minutes after addition of 10 uM CNQX, 50uM APV, and 100 uM picrotoxin or bicuculline (to inhibit AMPA, NMDA, and GABA receptors, respectively), the average transient frequency was 0.020 ± 0.012 (*Figure 8*). The frequency of transients in the Antagonists condition is significantly reduced from Baseline (*mean difference*: 0.023, $t = 2.1348$, $df = 27$, *p-value* = 0.042). The average transient frequency after 30-60 minutes of washout was 0.025 ± 0.025 (*Figure 8*). This group showed no significant difference between the Antagonists (*p-value = 0.6094*) or Baseline (*p-value = 0.2795*). These results suggest an effect of the antagonists on calcium transients, but the ability of transients to recover upon washout is inconclusive.

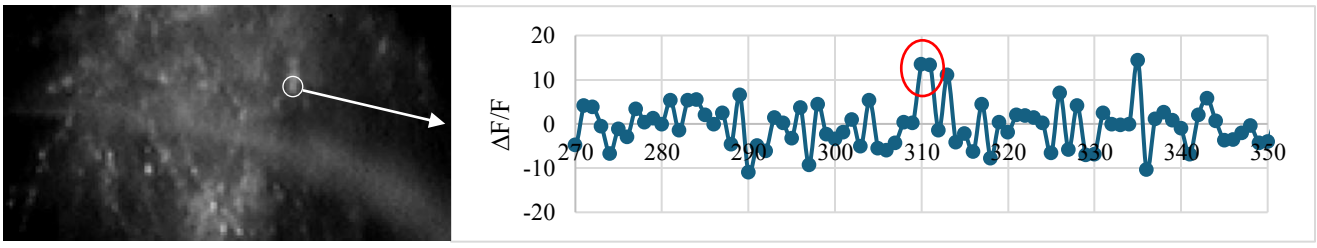

Figure 7 – Representative ROI trace of cytoplasmic calcium fluorescence
80-frame section of 2-minute (600 frame) ΔF/F trace for a single ROI labeled with Calcium Green Dextran at baseline without antagonists. Note the two consecutive data points (311-312) with values exceeding the threshold of 2.6 standard deviations, indicating a significant calcium transient.

A

Cytoplasmic Calcium			
	Baseline	Antagonists	Washout
Cord 1	0.044		
Cord 2	0.038	0.025	
Cord 3	0.000		
Cord 4	0.050		
Cord 5a	0.050	0.033	0.050
Cord 5b	0.075	0.017	0.000
Cord 6	0.025	0.006	0.025
Mean	0.040	0.020	0.025
Median	0.044	0.021	0.025
STDEV	0.023	0.012	0.025
p-value	**0.042**		
		0.6094	
			0.2795

B

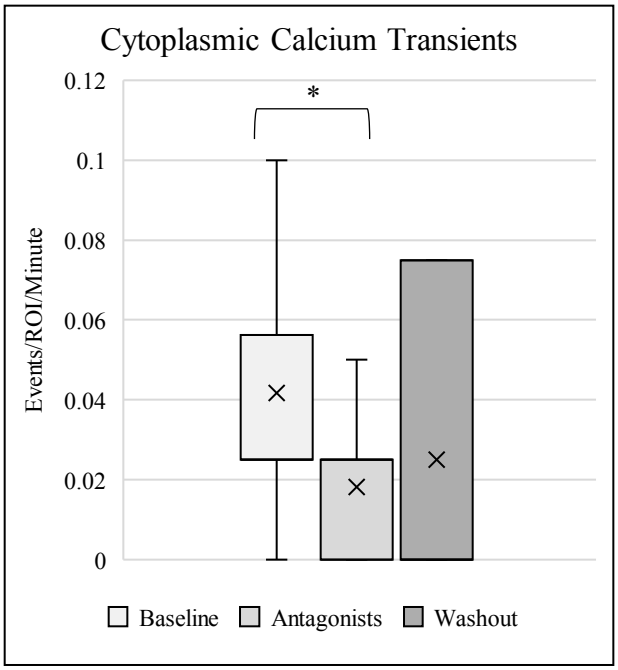

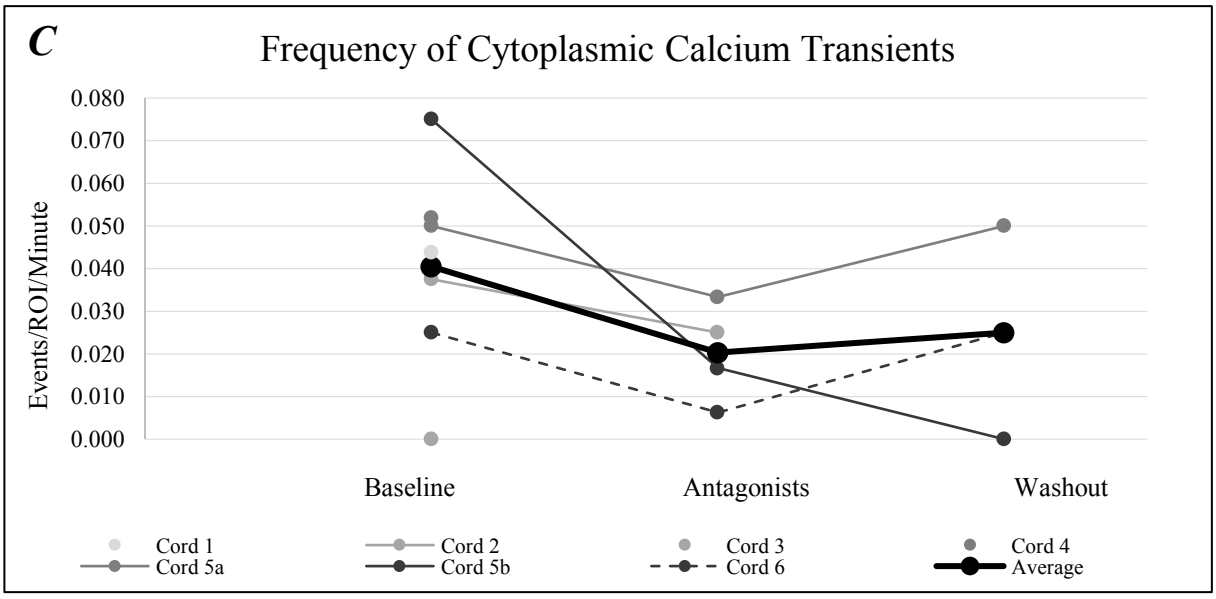

Figure 8 – Frequency of cytoplasmic calcium transients

*A) Table of average cytoplasmic calcium transient frequency per experimental group. B) Box and whisker plot of transient frequency (*p-value < 0.05). C) Scatterplot of average cytoplasmic calcium transient frequency per cord per experimental condition. A-C) The frequency decreased from baseline after addition of the antagonists (mean difference: 0.023, t = 2.1348, df = 27, p-value = 0.042). No significant difference was detected between the Antagonists group and the Washout group (p-value = 0.6094) or between Baseline and Washout (p-value = 0.2795).*

Mitochondrial Calcium

3 trials were conducted using cords that were electroporated with mito-GCaMP6f and dendritic calcium was imaged for mitochondrial calcium fluorescence (*Figure 10*). The average mitochondrial calcium transient frequency at baseline was 0.048 ± 0.034 events per ROI per minute. 30-60 minutes after CNQX, APV, and picrotoxin or bicuculline, the average transient frequency was 0.033 ± 0.036. The average transient frequency after 30-60 minutes of washout was 0.028 ± 0.021. While the frequency appeared to decrease from baseline after addition of the antagonists, no significant difference was detected between any of the experimental groups.

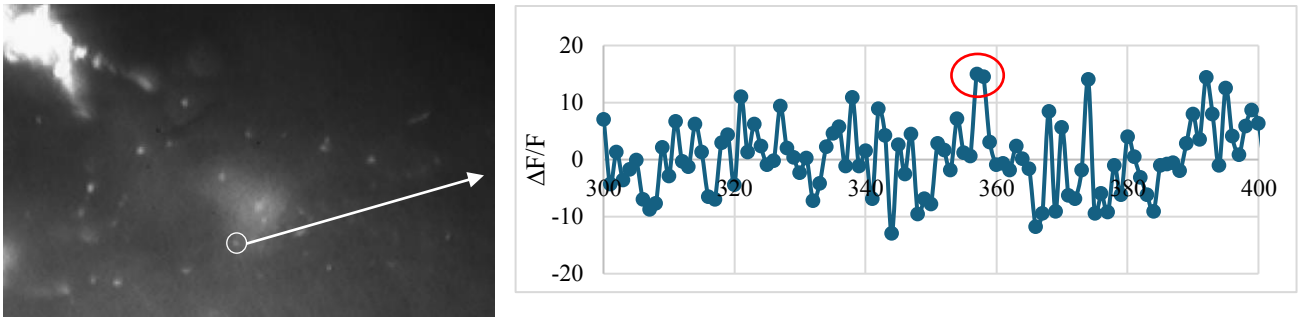

Figure 9– Representative ROI trace of mitochondrial calcium fluorescence
100-frame section of 2-minute (600 frame) ΔF/F trace for a single ROI labeled with mito-GCaMP6f at baseline without antagonists. Note the two consecutive data points (357-358) with values exceeding the threshold of 2.6 standard deviations, indicating a significant calcium transient.

A

Mitochondrial Calcium			
	Baseline	Antagonists	Washout
Cord 1	0.075	0.060	
Cord 2	0.031	0.025	0.038
Cord 3	0.033	0.006	0.019
Mean	0.048	0.033	0.028
Median	0.050	0.025	0.025
STDEV	0.034	0.036	0.021
p-value	0.3381		
		0.7164	
			0.1718

B

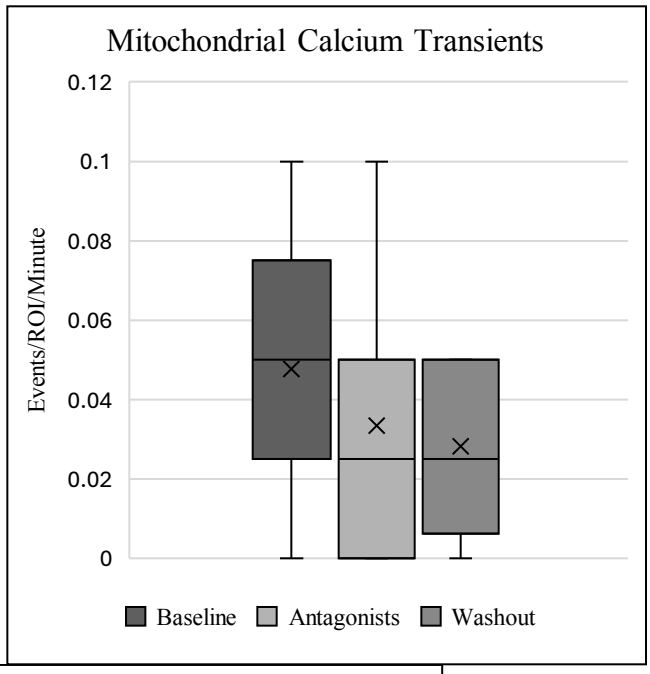

C

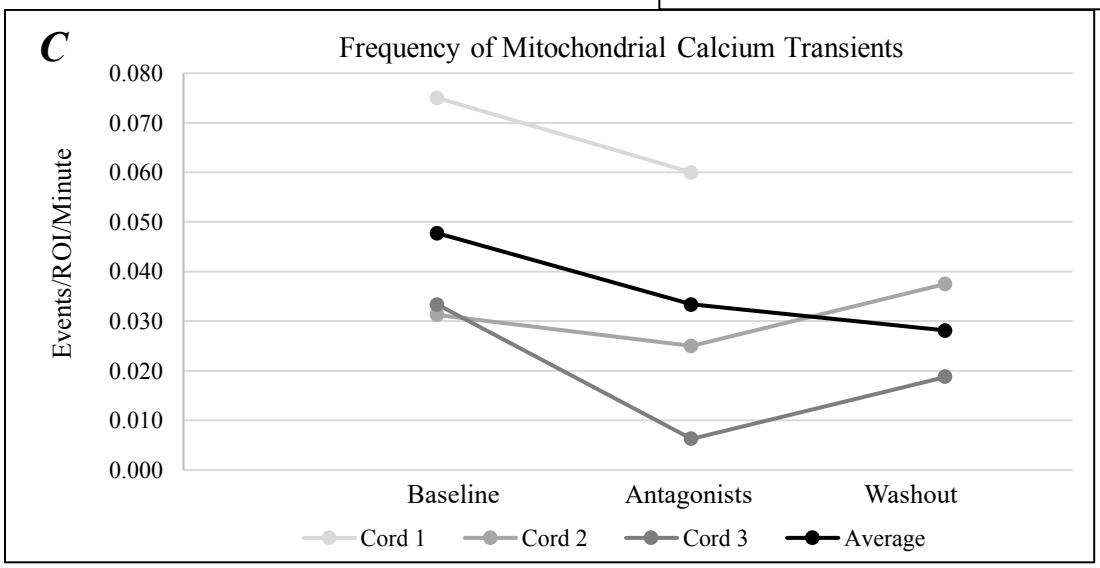

Figure 10 – Frequency of mitochondrial calcium transients
A) Table of average mitochondrial calcium transient frequency per experimental group. B) Box and whisker plot of mitochondrial calcium transient frequency. C) Scatterplot of average mitochondrial calcium transient frequency per cord per experimental condition. A-C) No significant difference was detected between any of the experimental groups (Baseline and Antagonists: p-value = 0.3381, Antagonists and Washout: p-value = 0.7164, Baseline and Washout: p-value = 0.1718).

Discussion

This is the first study to investigate calcium transients induced by miniature post-synaptic currents in embryonic chick spinal motoneurons. GABA, AMPA, and NMDA receptor antagonists were applied to measure the role of these receptors' activation in calcium transients that trigger synaptic scaling. Cytoplasmic calcium transients showed a significant reduction in response to these receptor antagonists. Mitochondrial calcium showed a non-significant trend downward. It is possible that the mitochondria have alternate sources of calcium that inhibited the effect of receptor blockade, but additional trials are needed to confidently conclude an effect.

The significant reduction of cytoplasmic calcium fluorescence upon inhibition of these receptors provides further evidence that one, all, or a combination of these receptors serve as essential sources of calcium in this system. It has been previously established that blockade of GABAergic and NMDAergic minis can cause slow and rapid synaptic scaling in this system, respectively. The results of this study provide further support for the theoretical scaling mechanism including mini-induced calcium. Given the evidence for calcium as the substrate that mediates scaling, further studies can target specific channels and receptors to identify the critical source of calcium.

In both cytoplasmic and mitochondrial calcium experiments, the frequency of calcium transients was not significantly different after washout than during antagonism or at baseline. This leads to conflicting conclusions about whether the calcium transients fully recover after washout. Additionally, the timing classification of the washout condition may not align with the exact time that the drugs are fully removed from the system. It is possible that the drugs do not fully wash out in the given time period, causing data from the "washout" period to still reflect an effect of the drugs.

Another limitation of the study includes the likelihood that some transients fell below our ability to detect them and that some events were not real transients. Regardless, we did achieve statistical significance in the reduction of transients following receptor antagonists.

Future studies should replicate this protocol with antagonism of only one receptor type at a time. A next direction would be to inhibit NMDARs only using APV. This would provide critical insight into the mechanism of rapid NMDA-induced scaling described by Pekala & Wenner (2022). If successful, a next step would be to target individual NDMAR subunits. Pekala et al. (unpublished) have identified the GluN2C/D NDMAR subunit as critical in the rapid scaling process. Future studies should test if blocking this subunit reduces calcium transients.

While this study suggests a potential role of GABA, AMPA, or NMDA receptors in calcium transients related to synaptic scaling, their exact role is still unclear. It is possible that scaling requires coincident GABAergic depolarization and NMDAR activation to induce scaling. GABAergic activation may cause a depolarization that then allows for the opening of either NDMAR or voltage-gated channels and calcium influx. However, findings from Reese and Kavalali (2015) indicate that voltage-gated calcium channels are not critical for mini-induced calcium transients involved in scaling in the hippocampus.

Another future direction would be to repeat this study with magnesium concentrations typical for this biological system. While canonical NMDARs require depolarization to remove the Mg^{2+} block, recent evidence suggests a possibility of NMDAR activation independent of Mg^{2+} concentration. Reese and Kavalali (2015) found that Mg^{2+} concentration did not affect mSCT amplitude or frequency. However, this was done in rat hippocampal cultures and has not been replicated in this system. The artificial reduction in magnesium concentration hinders the ability to interpret how the results of this study apply to the naturally occurring system. Further studies

should investigate calcium transients through each of these receptors at varying magnesium concentrations.

Identifying the source of calcium is only one step in elucidating the mechanism of synaptic scaling. Once calcium is in the cell, it could undergo multiple biochemical pathways that may mediate the scaling process. Two main pathways have been suggested to be involved in rapid scaling. The first of these pathways involves calcium interacting with eEF2 kinase. Calcium activates eEF2K, which inhibits protein translation via phosphorylation and inhibition of eukaryotic elongation factor 2 (eEF2), ultimately inhibiting the production of new AMPA receptors (Reese and Kavalali, 2015). The second pathway, proposed by Aoto et al. (2008), involves retinoic acid (RA). Aoto showed that blocking neuronal activity, specifically NMDA minis, increased RA synthesis, leading to increased expression of GluA1-containing AMPA receptors. This mechanism is suggested to involve calcineurin, a calcium-binding protein, which inhibits retinoic acid synthesis (Arendt et al., 2015).

It remains unclear whether mitochondria are involved in either of these pathways. Reese and Kavalali (2015) suggest that scaling involves a calcium-induced release of internal calcium stores, which could come from the endoplasmic reticulum or mitochondria. Pekala (unpublished) found that blocking calcium flow through the mitochondrial calcium uniporter did induce scaling. Mitochondria may be involved in sensing calcium transients, but the results from this study are inconclusive. Further experiments are needed to determine the role of mitochondria in synaptic scaling.

Conclusion

This study opens a new avenue for identifying the molecular mechanism that causes homeostatic scaling in the chick embryo. We were able to visualize calcium transients induced by miniature GABAergic or glutamatergic post-synaptic currents. Further, we demonstrated that these transients were reduced by the blockade of GABA, AMPA, and NMDA receptor activity, suggesting one or all these receptors act as the source of calcium involved in the scaling mechanism. Results are inconclusive regarding the impact of receptor blockade on mitochondrial calcium and the recovery of calcium transients upon antagonist washout. Future studies should build upon these findings to identify the specific receptors contributing to these calcium transients as well as the role of mitochondria and compare these results to their ability to trigger scaling.

References

Arendt, K. L., Zhang, Z., Ganesan, S., Hintze, M., Shin, M. M., Tang, Y., ... & Chen, L. (2015). Calcineurin mediates homeostatic synaptic plasticity by regulating retinoic acid synthesis. Proceedings of the National Academy of Sciences, 112(42), E5744-E5752.

Ashrafi, G., de Juan-Sanz, J., Farrell, R. J., & Ryan, T. A. (2020). Molecular Tuning of the Axonal Mitochondrial Ca2+ Uniporter Ensures Metabolic Flexibility of Neurotransmission. Neuron, 105(4), 678–687.e5.

Aoto, J., Nam, C. I., Poon, M. M., Ting, P., & Chen, L. (2008). Synaptic signaling by all-trans retinoic acid in homeostatic synaptic plasticity. Neuron, 60(2), 308-320.

Conrad, K. L., Tseng, K. Y., Uejima, J. L., Reimers, J. M., Heng, L. J., Shaham, Y., ... & Wolf, M. E. (2008). Formation of accumbens GluR2-lacking AMPA receptors mediates incubation of cocaine craving. *Nature*, *454*(7200), 118-121.

Dedhar, S., Rennie, P. S., Shago, M., Hagesteijn, C. Y. L., Yang, H., Filmus, J., ... & Giguère, V. (1994). Inhibition of nuclear hormone receptor activity by calreticulin. Nature, 367(6462), 480-483.

Desai, D., Michalak, M., Singh, N. K., & Niles, R. M. (1996). Inhibition of retinoic acid receptor function and retinoic acid-regulated gene expression in mouse melanoma cells by calreticulin. A potential pathway for cyclic AMP regulation of retinoid action. The Journal of biological chemistry, 271(25), 15153–15159. https://doi.org/10.1074/jbc.271.25.15153

Fong, M. F., Newman, J. P., Potter, S. M., & Wenner, P. (2015). Upward synaptic scaling is dependent on neurotransmission rather than spiking. Nature communications, 6(1), 6339.

Frere, S., & Slutsky, I. (2018). Alzheimer's disease: from firing instability to homeostasis

network collapse. *Neuron*, *97*(1), 32-58.

Garcia-Bereguiain, M. A., Gonzalez-Islas, C., Lindsly, C., Butler, E., Hill, A. W., & Wenner, P. (2013). In vivo synaptic scaling is mediated by GluA2-lacking AMPA receptors in the embryonic spinal cord. Journal of Neuroscience, 33(16), 6791-6799.

Garcia-Bereguiain, M. A., Gonzalez-Islas, C., Lindsly, C., & Wenner, P. (2016). Spontaneous release regulates synaptic scaling in the embryonic spinal network in vivo. Journal of Neuroscience, 36(27), 7268-7282.

Gogolla, N., LeBlanc, J. J., Quast, K. B., Südhof, T. C., Fagiolini, M., & Hensch, T. K. (2009). Common circuit defect of excitatory-inhibitory balance in mouse models of autism. Journal of neurodevelopmental disorders, 1, 172-181.

Gonzalez-Islas, C., Sabra, Z., Fong, M. F., Yilmam, P., Yong, N. A., Engisch, K., & Wenner, P. (2024). GABAergic synaptic scaling is triggered by changes in spiking activity rather than AMPA receptor activation. Elife, 12, RP87753.

Hamburger, V., & Hamilton, H. L. (1951). A series of normal stages in the development of the chick embryo. Journal of morphology, 88(1), 49-92.

Hou, Q., Zhang, D., Jarzylo, L., Huganir, R. L., & Man, H. Y. (2008). Homeostatic regulation of AMPA receptor expression at single hippocampal synapses. Proceedings of the National Academy of Sciences, 105(2), 775-780.

Kavalali, E. T., & Monteggia, L. M. (2020). Targeting homeostatic synaptic plasticity for treatment of mood disorders. *Neuron*, *106*(5), 715-726.

Lim, Y. H., Licari, M., Spittle, A. J., Watkins, R. E., Zwicker, J. G., Downs, J., & Finlay-Jones, A. (2021). Early motor function of children with autism spectrum disorder: a systematic review. Pediatrics, 147(2).

Newport, D. J., Carpenter, L. L., McDonald, W. M., Potash, J. B., Tohen, M., Nemeroff, C. B., & APA Council of Research Task Force on Novel Biomarkers and Treatments. (2015). Ketamine and other NMDA antagonists: early clinical trials and possible mechanisms in depression. American Journal of Psychiatry, 172(10), 950-966.

Pekala, D., & Wenner, P. (2022). The uniform and nonuniform nature of slow and rapid scaling in embryonic motoneurons. Journal of Neuroscience, 42(7), 1224-1234.

Reese, A. L., & Kavalali, E. T. (2015). Spontaneous neurotransmission signals through store-driven Ca2+ transients to maintain synaptic homeostasis. Elife, 4, e09262.

Styr, B., Gonen, N., Zarhin, D., Ruggiero, A., Atsmon, R., Gazit, N., ... & Slutsky, I. (2019). Mitochondrial regulation of the hippocampal firing rate set point and seizure susceptibility. Neuron, 102(5), 1009-1024.

Südhof, T. C. (2008). Neuroligins and neurexins link synaptic function to cognitive disease. *Nature*, *455*(7215), 903-911.

Sutton, M. A., Ito, H. T., Cressy, P., Kempf, C., Woo, J. C., & Schuman, E. M. (2006). Miniature neurotransmission stabilizes synaptic function via tonic suppression of local dendritic protein synthesis. Cell, 125(4), 785-799.

Turrigiano, G. G., Leslie, K. R., Desai, N. S., Rutherford, L. C., & Nelson, S. B. (1998). Activity-dependent scaling of quantal amplitude in neocortical neurons. Nature, 391(6670), 892-896.

Wenner, P. A. (2020). Development of the locomotor system—chick embryo. In The Neural Control of Movement (pp. 221-236). Academic Press.

Wilhelm, J. C., & Wenner, P. (2008). GABAA transmission is a critical step in the process of triggering homeostatic increases in quantal amplitude. Proceedings of the National

Academy of Sciences, 105(32), 11412-11417.

Zhang, Z., Marro, S. G., Zhang, Y., Arendt, K. L., Patzke, C., Zhou, B., ... & Chen, L. (2018). The fragile X mutation impairs homeostatic plasticity in human neurons by blocking synaptic retinoic acid signaling. *Science translational medicine*, *10*(452), eaar4338.

Zoghbi, H. Y. (2003). Postnatal neurodevelopmental disorders: meeting at the synapse?. Science, 302(5646), 826-830.